Mon. Not. R. Astron. Soc. **390,** 1061–1070 (2008) doi:10.1111/j.1365-2966.2008.13774.x

A bright, dust-obscured, millimetre-selected galaxy beyond the Bullet Cluster (1E0657−56)

G. W. Wilson,[1⋆] D. H. Hughes,[2] I. Aretxaga,[2] H. Ezawa,[3] J. E. Austermann,[1] S. Doyle,[4] D. Ferrusca,[5,2] I. Hernández-Curiel,[2,6] R. Kawabe,[3] T. Kitayama,[7] K. Kohno,[8] A. Kuboi,[3] H. Matsuo,[3] P. D. Mauskopf,[4] Y. Murakoshi,[7] A. Montaña,[2] P. Natarajan,[9] T. Oshima,[3] N. Ota,[10,11] T. A. Perera,[1] J. Rand,[1] K. S. Scott,[1] K. Tanaka,[8] M. Tsuboi,[10] C. C. Williams,[1] N. Yamaguchi[3] and M. S. Yun[1]

[1]*Department of Astronomy, University of Massachusetts, Amherst, MA 01003, USA*
[2]*Instituto Nacional de Astrofísica, Óptica y Electrónica, Tonantzintla, Aptdo. Postal 51 y 216, 72000 Puebla, Pue., Mexico*
[3]*National Astronomical Observatory of Japan, 2-21-1 Osawa, Mitaka, Tokyo 181-8588, Japan*
[4]*Department of Physics and Astronomy, Cardiff University, Cardiff CF24 3YB*
[5]*Department of Physics, University of California, Berkeley 94720-7300, USA*
[6]*Centro de Radioastronomía y Astrofísica, Universidad Nacional Autónoma de México, Aptdo. Postal 72-3 (Xangari), 58089 Morelia, Mexico*
[7]*Department of Physics, Toho University, Funabashi, Chiba 274-8510, Japan*
[8]*Institute of Astronomy, The University of Tokyo, 2-21-1 Osawa, Mitaka, Tokyo 181-0015, Japan*
[9]*Department of Physics, Yale University, New Haven, CT 06520-208120, USA*
[10]*Institute of Space and Astronautical Science, JAXA, 3-1-1 Yoshinodai, Sagamihara, Kanagawa 229-8510, Japan*
[11]*Max-Planck-Institut für extraterrestrische Physik, Giessenbachstrasse, 85748 Garching, Germany*

Accepted 2008 July 29. Received 2008 July 24; in original form 2008 March 24

ABSTRACT

Deep 1.1 mm continuum observations of 1E0657−56 (the 'Bullet Cluster') taken with the millimeter-wavelength camera AzTEC on the 10-m Atacama Submillimeter Telescope Experiment (ASTE), have revealed an extremely bright ($S_{1.1\,\mathrm{mm}} = 15.9$ mJy) unresolved source. This source, MMJ065837−5557.0, lies close to a maximum in the density of underlying mass distribution, towards the larger of the two interacting clusters as traced by the weak-lensing analysis of Clowe et al. Using optical–infrared (IR) colours, we argue that MMJ065837−5557.0 lies at a redshift of $z = 2.7 \pm 0.2$. A lensing-derived mass model for the Bullet Cluster shows a critical line (caustic) of magnification within a few arcsec of the AzTEC source, sufficient to amplify the intrinsic millimetre-wavelength flux of the AzTEC galaxy by a factor of $\gg$20. After subtraction of the foreground cluster emission at 1.1 mm due to the Sunyaev-Zel'dovich effect, and correcting for the magnification, the rest-frame far-IR luminosity of MMJ065837−5557.0 is $\leq 10^{12}$ L$_\odot$, characteristic of a luminous infrared galaxy (LIRG). We explore various scenarios to explain the colours, morphologies and positional offsets between the potential optical and IR counterparts, and their relationship with MMJ065837−5557.0. Until higher resolution and more sensitive (sub)millimetre observations are available, the detection of background galaxies close to the caustics of massive lensing clusters offers the only opportunity to study this intrinsically faint millimetre-galaxy population.

Key words: galaxies: high-redshift – galaxies: starburst.

1 INTRODUCTION

A high redshift ($z \gg 1$) strongly evolving submillimetre-galaxy population (hereafter SMGs) has been identified in a series of continuum imaging surveys during the last decade. The most significant surveys have been undertaken with Submillimetre Common-User Bolometer Array (SCUBA) at 850 μm (Coppin et al. (2006) and references therein), MAMBO at 1.2 mm (Greve et al. 2004; Bertoldi et al. 2007), BOLOCAM (Laurent et al. 2005) at 1.1 mm, and more recently with AzTEC at 1.1 mm (Scott et al. 2008). These collective submillimetre surveys, together with comprehensive multi-wavelength imaging and spectroscopic follow-up spanning X-ray to radio wavelengths, have demonstrated that SMGs are representative

⋆E-mail: wilson@astro.umass.edu

of a population of massive, dust enshrouded, optically faint galaxies undergoing significant star formation with rates $\gg$200 $M_\odot$ yr^{-1}. The median redshift of the bright SMG population, based on spectroscopic and photometric redshifts, is $\sim$2.5, with approximately 50 per cent of the population at $1.9 < z < 2.9$ (Aretxaga et al. 2003; Chapman et al. 2003, 2005; Pope et al. 2005; Aretxaga et al. 2007). Scaling the observed flux densities of all SMGs with detections in the above flux-limited surveys to 850 μm, the majority of the population have been detected with flux densities of $2 < S_{850\,\mu m} < 12$ mJy.

Making the connection between ultra-luminous SMGs and their local analogs – presumably ultra-luminous infrared galaxies (ULIRGS) and luminous infrared galaxies (LIRGS) – requires either larger telescopes such as the Large Millimetre Telescope (LMT) and the Atacama Large Millimetre Array (ALMA) or using the presence of foreground structure to amplify the faint background galaxies. To date, the deepest SMG surveys have been conducted towards lensing clusters that amplify an intrinsically fainter population of SMGs in the high-z universe (Smail, Ivison & Blain 1997; Chapman et al. 2002; Cowie, Barger & Kneib 2002; Smail et al. 2002; Kneib et al. 2004; Knudsen et al. 2006). Imaging massive clusters offer the advantages of amplification of the background universe due to the gravitational potential of the cluster and, in general, an increased effective resolution in the source plane (and correspondingly decreased survey confusion limit). Unfortunately, this same advantage for those studying faint background galaxies comes at a cost to those interested in studying the clusters themselves using the Sunyaev–Zel'dovich Effect (SZE). The amplified (sub)millimetre-wavelength emission from members of the SMG field population that are lensed by the large-scale cluster potential and by the increased probability of galaxy–galaxy lensing along the line of sight to the cluster, increases the likelihood of point-source contamination of the SZE.

In this paper, we present the discovery of an extremely bright millimetre-selected SMG (MMJ065837−5557.0) in the direction of the massive X-ray luminous Bullet Cluster ($z = 0.297$). The 1.1 millimetre-wavelength observations were made with the AzTEC instrument (Wilson et al. 2008) on the Atacama Submillimeter Telescope Experiment (ASTE, Ezawa et al. 2004). These AzTEC data were undertaken as part of a larger project to trace the evolution in the surface density of SMGs towards overdense regions in the low- and high-redshift Universe. Using archival *Hubble Space Telescope* (*HST*) and *Spitzer* data, we identify potential optical and infrared (IR) counterparts to the AzTEC source. The photometric colours, and the small positional offset of the AzTEC source and the optical–IR counterparts from the critical magnification line derived from cluster mass models strongly support the suggestion that MMJ065837−5557.0 is a moderately luminous high-z galaxy that has been lensed and amplified by the massive foreground Bullet Cluster.

Throughout this paper, we adopt the following cosmological model: a Hubble constant $H_0 = 72$ km s^{-1} Mpc^{-1}, and density parameters $\Omega_M = 0.3$ and $\Omega_\Lambda = 0.7$.

2 AZTEC/ASTE OBSERVATIONS

AzTEC is a 144-element bolometric receiver currently tuned to operate in the 1.1 mm atmospheric window (Wilson et al. 2008). We have previously used AzTEC to complete a successful set of observations of the submillimetre galaxy population in blank fields from the 15 m diameter James Clerk Maxwell Telescope (e.g. Perera et al. 2008; Scott et al. 2008; Austermann et al, in preparation). In 2007, AzTEC was mounted on the ASTE telescope, a 10 m diameter antenna located on Pampa La Bola, near Cerro Chajnantor in Chile. ASTE provides AzTEC with an angular resolution of 30 arcsec full width at half-maximum (FWHM). One season of observations (2007 June–October) from this excellent high ($\sim$4900 m) and dry site in the Atacama Desert has been completed and another season will begin in 2008 July.

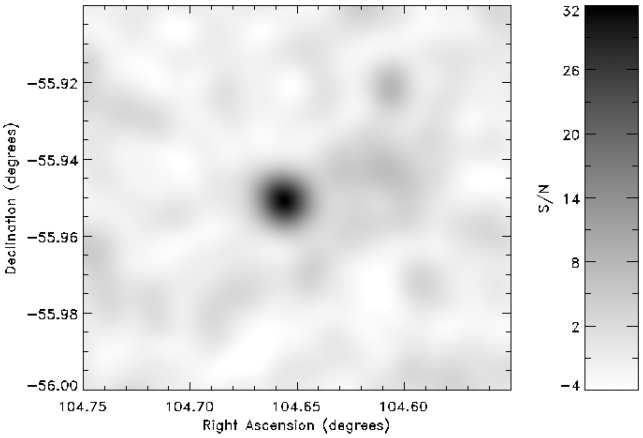

Figure 1. AzTEC image of MMJ065837−5557.0. The colour bar shows the shading in units of signal-to-noise of a point-source detection. The underlying noise in the map varies by 4.6 per cent across the portion of the image shown. The faint diffuse emission to the west of the point source is dominated by the extended SZE signal from the Bullet Cluster (Ezawa et al. in preparation), however, due to the point-source filtering of the map, no morphological information about the SZE should be taken from this figure.

The bright millimetre-wavelength source, shown in Fig. 1, was found in our 202 arcmin^2 AzTEC imaging survey of the Bullet Cluster and its environment (Ezawa et al., in preparation). Observations were made by continuously scanning the telescope boresight in azimuth and elevation in a modified Lissajous pattern centred on $06^h\,58^m29\overset{s}{.}40$, $-55^d\,56^m\,42\overset{s}{.}0$. The modified Lissajous pattern is defined as a function of time, t, by

$$\delta\mathrm{Az} = A \sin at + B \sin at/30$$

$$\delta\mathrm{El} = A \sin bt + B \sin bt/30$$

where $A = 5.5$ arcmin, $B = 2$ arcmin, $a/b = 8/9$, and δAz and δEl are physical coordinates relative to the field centre. The actual values of a and b are normalized to limit the peak telescope velocity to 300 arcsec s^{-1}. A total of 61 maps of the cluster were completed, each taking 41.7 min, and collectively yielding an equivalent total on-source integration time of 193 s per 3 × 3 arcsec^2 pixel. The data are reduced and co-added using the standard AzTEC data analysis pipeline with very similar techniques to those described in Scott et al. (2008). The resultant map has an average point-source flux error of 0.54 mJy over the inner 150 arcmin^2 area. A full analysis of the extended 1.1 mm Sunyaev–Zel'dovich emission of the cluster and other point sources in the map will be presented in subsequent papers.

2.1 Pointing corrections and source position

A small correction to the telescope pointing model is applied to all observations of the Bullet Cluster field based on periodic observations of a bright point source, PKS 0537−441, with a 1.1 mm flux of $\sim$5 Jy. We derived the correction by linearly interpolating the pointing offsets measured from 4 × 4 arcmin^2 maps of the point

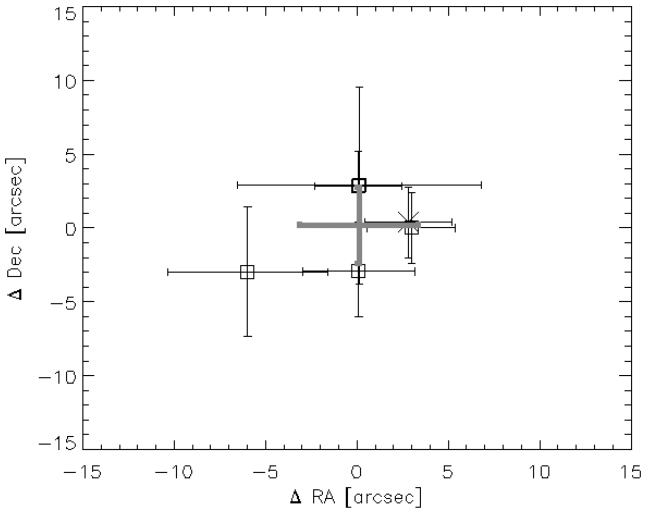

Figure 2. Measured positional offsets determined from maps of five high-redshift radio galaxies (squares) and by stacking radio-detected AzTEC sources in the GOODS-S field (×). Error bars represent the 1 σ uncertainty in the centroid of the 1.1 mm flux of the radio galaxies. The red thick cross denotes the mean offset of the fields with bar lengths equal to the square root of the weighted variance of the set of radio galaxy offsets.

source observed every 2 h. Pointing measurements always bracketed observations of the cluster. Our resulting pointing uncertainty, as measured from stacking the 1.1 mm flux at the locations of 212 known radio sources in our map of the GOODS-S field (using the technique described in Scott et al. (2008)) is 4.8 arcsec rms. This is a random pointing error which broadens the point spread function (PSF) of the instrument by less than 0.5 arcsec and suppresses the point source response by an amount that is negligible compared to the photometric error.

To identify the correct optical/IR counterpart to MMJ065837−5557.0 we next check for any systematic offset in the pointing, which could be mechanical in nature or could be due to environmental influences on the telescope at the time of the observation. In either case, systematic offsets are likely to vary from field to field. Without a known millimetre-bright object in our Bullet Cluster map to use as a pointing reference (or a sufficient number of fainter objects spread throughout the field to allow a stacking analysis) there is no way to determine any astrometric offset specific to this field. Instead, we estimate our overall astrometric uncertainty as the variance in residual pointing offsets (after the corrections applied from our observations of PKS 0537−441) measured from similar maps of five high-redshift radio galaxies, along with the offsets measured from the stacking analysis from the GOODS-S field. Fig. 2 shows the measured offsets in right ascension and declination (physical coordinates) from these data. The thick red cross at ΔRA, ΔDec. = (0.″10, 0.″18) shows the mean offset and 1σ errors (3.″24 in RA and 2.″61 in Dec.), that is consistent with no systematic specific offset. Hence, in the analysis and discussion that follows, we apply no offset correction to the derived centroid of the point source. We assume that the standard deviation of systematic pointing offsets measured in other AzTEC maps, taken in a similar manner to the Bullet Cluster data, is representative of any positional offsets.

To get the most accurate centroid position for MMJ065837−5557.0, we fit a two-dimensional Gaussian to the unfiltered image of the source. In addition to the source position we fit for an amplitude, the semi-major and semi-minor axes and position angle of the ellipse, and an arbitrary constant offset. Fitted parameters and their statistical errors are given in Table 1.

Table 1. Derived parameters for MMJ065837−5557.0. The absolute calibration error of the flux density is given in parentheses.

Flux density	15.9 ± 0.5 (± 1.3) mJy
SZE-corrected flux density	13.5 ± 0.5 (± 1.0) mJy
RA centroid position	06:58:37.31 $\pm$ 0.02 s
Dec. centroid position	−55:57:01.5 $\pm$ 0.32 arcsec
Source FWHM (RA)	36 ± 1.3 arcsec
Source FWHM (Dec.)	32 ± 1.2 arcsec
Position angle of elongation	$34^\circ \pm 8^\circ$
reduced χ^2/ of fit	0.94

2.2 Calibration and flux determination

The AzTEC Bullet Cluster data are calibrated using Uranus as a primary calibrator and adopting the technique described in Wilson et al. (2008). Beammaps of Uranus were made twice each night. A linearly interpolated calibration factor is applied to Bullet Cluster observations taken between Uranus beammaps. The calibration factor derived from the nearest Uranus beammap in time is used for Bullet Cluster observations taken before the first Uranus beammap of the evening and for Bullet Cluster observations taken following the last Uranus beammap of the evening. Since most of the science observations took place following the last Uranus beammap of the evening, we estimate an upper limit to our overall calibration uncertainty from the standard deviation in reported fluxes from 31 pointing observations of PKS 0537−441, which is 6 per cent. PKS 0537−411 is known to be a strongly varying source (Romero, Combi & Colomb 1994) and so this upper limit should be considered robust. Adding this in quadrature with the 5 per cent uncertainty in the brightness temperature of Uranus at 1.1 mm (Griffin & Orton 1993) gives a total calibration error of 8 per cent.

We use the two-dimensional Gaussian fit described above to estimate the flux density of MMJ065837−5557.0 in the absence of any foreground SZE emission from the cluster. Since the AzTEC map has been Wiener filtered to optimally identify point sources, an unknown degree of attenuation has been applied to the extended SZE signal. Thus the fitted point-source flux density, allowing for a lower limit on the contribution of SZE, is $S_{1.1\,\mathrm{mm}} = 13.5 \pm 0.5$ (± 1.0) mJy where the first error is the statistical error and the second (in parentheses) is the error in absolute calibration.

The fitted size of MMJ065837−5557.0 is larger and slightly elongated compared to the beam size measured by performing the same fit to the 31 observations of the point-source PKS0537−441 (FWHM = 29 $\pm$ 1.2 arcsec), suggesting that the flux of MMJ065837−5557.0 may be due to a close pair, or possibly triplet (see Section 3.5), of confused sources. Until we have performed a more detailed subtraction of the SZE emission, or undertaken higher resolution observations, we cannot rule out that the flux from MMJ065837−5557.0 is from a single point source.

3 DISCUSSION

A comparison with the measured surface density of SMGs detected towards wide-area blank fields (e.g. Coppin et al. 2006; Scott et al. 2008, and references therein) is sufficient to demonstrate how unexpected is the detection of such a bright source. Although the submillimetre source counts are unconstrained at these brightness levels, a wide-area survey of $\gg 1\,\mathrm{deg}^2$ is necessary before such

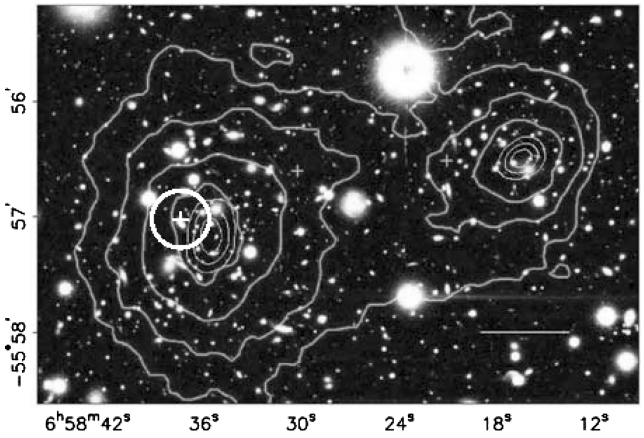

Figure 3. The weak-lensing map (green contours), from Clowe et al. (2006) of the Bullet Cluster overlaid on an optical image that shows the two merging clusters of galaxies, with the less-massive 'Bullet' subcluster to the west of the main cluster. The white contours towards the peaks of the mass distribution indicate their positional uncertainty. The position of the bright AzTEC source MMJ065837−5557.0, which lies close to the peak of the more massive cluster, is shown as a white cross. The white circle indicates the scale of the AzTEC beam with 30 arcsec diameter FWHM. The full AzTEC map is significantly larger than the area of the optical image shown here.

an intrinsically bright object could be expected to be discovered in a random survey. Two other similarly bright sources have been found in previous SCUBA surveys: J02399−0136, with an observed 850 μm flux density of 26 ± 3 mJy due to the amplification by the massive cluster Abell 370 at $z = 0.37$ (Ivison et al. 1998); and the high-redshift radio galaxy 8C1909+722 which shows extended submillimetre emission and has an integrated flux of 34.9 ± 3 mJy at 850 μm (Stevens et al. 2003).

Given that MMJ065837−5557.0 has been detected near the peak in the weak-lensing map associated with the more massive of the two merging clusters (see Fig. 3), and that the Bullet Cluster shows optical signatures (i.e. arcs) of strong lensing, magnification of this source and amplification of the (sub)millimetre fluxes is a natural explanation of the high apparent brightness. Due to the low spatial resolution of these single-dish ASTE observations (30 arcsec FWHM at 1.1 mm) and the astrometric uncertainty, however, we must consider and dismiss other alternatives for the source of the millimetre emission including Galactic stars, potential confusion with foreground Galactic cirrus or galaxies intrinsic to the cluster at $z = 0.297$.

3.1 Rejecting a Galactic origin for MMJ065837−5557.0

Within a 6.5 arcsec radius, 2σ positional error circle of the AzTEC source there is a compact point source at the resolution of *HST* (object S in Fig. 4). The object is identified as a star in the Naval Observatory Merged Astrometric Dataset (NOMAD). S has a *R*-band magnitude of 18.8, which corresponds to a flux density of 0.19 mJy. Assuming a blackbody photospheric spectrum ($T_{\rm eff} \sim 4500$ K) and that there is no extended circumstellar dust envelope, which is consistent with the declining flux density of object S from 3.6 to 8 μm in the corresponding *Spitzer* imaging (see Fig. 3), then S cannot be responsible for the 13.5 mJy emission at 1.1 mm. For completeness, we considered the possibility that the 'stellar object' S is an uncatalogued quasar at an unknown redshift. In the absence of an optical spectrum, we derive the IR colours of source S: $S_{8.0}/S_{4.5} < 0.40$, $S_{5.8}/S_{3.6} \sim 1.7$. Source S is bluer than a typical IR active galactic nucleus (AGN) and falls outside of the region of the colour–colour diagram shared by SMGs and AGN Yun et al. (2008). We therefore reject source S as the source of the millimetre flux.

At a Galactic latitude of $b \sim -21^\circ$ the foreground dust emission associated with Galactic cirrus is moderately weak in the vicinity of the Bullet Cluster, with a 100 μm surface brightness of ∼5 MJy sr^{-1}. Adopting the measured 60/100 μm cirrus colour temperature of ∼20 K (and a dust emissivity-index $\beta = 2$), we estimate that the contribution to the measured AzTEC 1.1 mm flux density is ∼1 mJy in the 30 arcsec FWHM beam. This estimate is sensitive to the exact temperature of the cirrus, and can increase to 5 mJy for colder cirrus

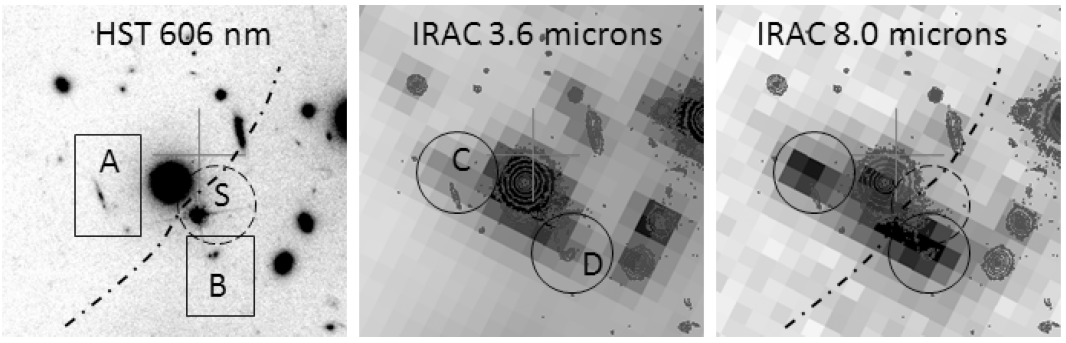

Figure 4. Left-hand panel: *HST* ACS image (606W filter) showing a field of 23 × 23 arcsec^2 centred on the centroid position (shown as a red cross) of MMJ065837−5557.0. The dimension of the cross indicates the $\pm 1\sigma$ positional uncertainty of 3 arcsec for MMJ065837−5557.0, which corresponds to a physical distance of ∼22 kpc for a galaxy at $2 < z < 3$. The dashed lines, shown only on the *HST* and IRAC 8.0 μm images, bisecting the two red-galaxy systems (A/C and B/D), and close to the position of the elliptical galaxy (E – a spectroscopically confirmed member of the Bullet Cluster), are the approximate locations of the critical line of infinite magnification for a galaxy at $z = 2.7$ (adapted from Gonzalez et al. 2008). A stellar object, S, is also identified. The optical galaxies A and B, enclosed within rectangles, are two candidates for highly lensed background sources that may be high-z counterparts to the AzTEC source MMJ065837−5557.0. The IRAC 3.6 μm (middle panel) and 8.0 μm (right-hand panel) images of the same field as the *HST* image are shown with optical contours overlaid. Clear colour differences and spatial displacements, given in Table 1, are seen between the optical components A and B, and the IR components C and D (shown as circles). Bradač et al. (2006) present an alternative mass model in which the critical line passes closer to object A. It requires higher resolution (sub)millimetre observations with ALMA to confirm which of these components (if any) is the counterpart to MMJ065837−5557.0. Optical–IR spectroscopy are required to show whether the galaxy systems A/C and B/D are multiple lensed images of the same background galaxy with heavy patchy dust obscuration, or if components A, B, C and D are separate galaxies involved in strong interactions that stimulate an episode of luminous star formation, or alternatively if they are physically unconnected galaxies in our line of sight.

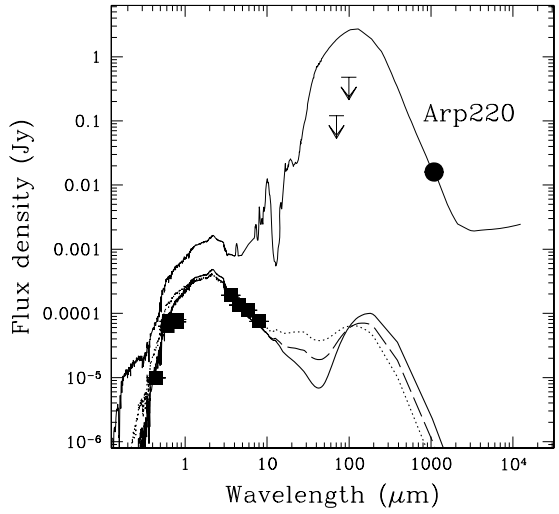

Figure 5. SED of the $z = 0.297$ cluster member galaxy E (Fig. 4) near the MMJ065837−5557.0 position centroid. The measured photometry data for the galaxy E are shown as filled squares, and they are compared with three elliptical galaxy SED templates by Polletta et al. (2007) with different ages (2, 5 and 13 Gyr old shown as dotted, dashed and solid lines, respectively). The two 3σ upper limits from the IRAS 60 and 100 μm bands are also shown. The Arp 220 SED by Polletta et al. is normalized to the 1.1 mm AzTEC measurement (filled circle) for comparison.

($T = 15$ K). However, the spatial filter applied during the AzTEC data reduction suppresses any extended foreground emission on scales much larger than the point source response and therefore acts as a local sky subtraction at the position of MMJ065837−5557.0. Unless the measured power due to cirrus is dominated by emission on angular scales smaller than 30 arcsec, foreground Galactic cirrus is unlikely to be responsible for the bright point-source emission of MMJ065837−5557.0. For the reasons given above, we confidently reject a Galactic origin for MMJ065837−5557.0.

3.2 Rejecting a cluster-member origin for MMJ065837−5557.0

The optical galaxy nearest to the AzTEC centroid is an elliptical galaxy, which is a spectroscopically confirmed member of the Bullet Cluster. Located only 1.5 arcsec from the AzTEC source location, this $B = 21.58$ elliptical galaxy at $z = 0.2958$ (Barrena et al. 2002) is a natural candidate for a counterpart to the 1.1 mm continuum emission. It is also the nearest and the brightest Infrared Array Camera (IRAC) source located within the 1σ positional uncertainty of MMJ065837−5557.0.

As shown in Fig. 5, both the optical and the IRAC near-IR data of the galaxy are completely consistent with the spectral energy distribution (SED) of a typical elliptical galaxy, dominated by a predominantly old stellar population. The predicted 1.1 mm flux density for such an elliptical galaxy, however, is nearly 4 orders of magnitudes smaller than that measured by AzTEC. However, major mergers of two gas-rich galaxies that lead to the ULIRG phenomenon are also known to produce an elliptical-like stellar remnant (Hibbard & Yun 1999). We explore the possibility that this elliptical galaxy may host a substantial and compact reservoir of cold gas and dust by plotting the SED of Arp 220 (a prototypical ULIRG) scaled to match the measured 1.1 mm flux density of MMJ065837−5557.0. The discrepancy between the observed flux density and the scaled Arp 220 SED is only a factor of a few in the optical bands, but the difference grows quickly and substantially at $\lambda > 1$ μm. The absence of the polycyclic aromatic hydrocarbon feature in the IRAC 8 μm band can be interpreted as evidence that the elliptical galaxy does not contain a large reservoir of cold gas and dust. This galaxy is not detected by the Infrared Astronomy Satellite (IRAS), and we show the 3σ upper limits of 120 and 480 mJy in the IRAS 60 and 100 μm bands[1] in Fig. 5. An Arp 220-like SED that can account for the measured 1.1 mm flux density can be ruled out with $>10\sigma$ significance. Therefore, we confidently reject the possibility that the elliptical galaxy is the origin of the extreme 1.1 mm continuum flux density of MMJ065837−5557.0.

We cannot confidently rule out other, more exotic alternative possibilities as the source of the bright millimetre emission such as nearby cooling-flow galaxies or exceptionally strong line emitters. As described below we instead focus on the most plausible explanation: two red IRAC sources (identified by Bradač et al. 2006 and further studied by Gonzalez et al. 2008) representing a background galaxy or galaxies magnified by the Bullet Cluster lens.

3.3 MMJ065837−5557.0 – a highly magnified, high-redshift starburst galaxy

The Bullet Cluster is a high-velocity merger ($\sim$4500 km s^{-1}) of two massive systems (the main cluster and the 'bullet' subcluster) of galaxies taking place in the plane of the sky. Although there is continued discussion regarding the exact mass ratio ($M_{\rm main}/M_{\rm bullet}$) of the two components ranging from 3:1 (Nusser 2008) to 10:1 (Barrena et al. 2002), the total dark-matter halo cluster mass is constrained to the range $\sim$0.8–2 $\times$ 10^{15} $M_\odot$ (Clowe et al. 2006; Vikhlinin et al. 2006). MMJ065837−5557.0 is within 15 arcsec of a peak in the underlying mass distribution of the main galaxy cluster and so a plausible scenario is that we are detecting amplified emission of a background source close to this position. Furthermore, the lensing models of Mehlert et al. (2001) and Gonzalez et al. (2008) show that critical lines (caustics) of infinite magnification for galaxies at $z = 3.24$ and 2.7, respectively, pass within a few arcsec of the centroid position of MMJ065837−5557.0 (Fig. 4). Thus, strong magnification of a background submillimetre galaxy is our preferred explanation for the unusual brightness of MMJ065837−5557.0. We now turn to the archival *HST* and IRAC data to identify the most likely counterparts of the millimetre-wavelength emission.

Fig. 4 shows a close-up view of the *HST* and IRAC fields near MMJ065837−5557.0, along with the approximate position of the lensing caustic line of infinite magnification. Having ruled out the elliptical galaxy closest to the AzTEC centroid as the source of the strong millimetre wavelength emission, we focus on the two reddest IRAC sources (labelled C and D in the IRAC 8 μm image of Fig. 4) that lie within the uncertainty of the AzTEC centroid position, and that are also bisected by the caustic line. The IRAC colours of objects C and D (see Table 2) are similar to those of dusty, optically obscured, high-redshift SMGs. Objects C and D also appear to be the same two galaxies identified by Bradač et al. (2006) as candidates for galaxies at $z > 6$ on the basis of their IR colours. We argue in Section 3.4 that objects C and D lie at significantly lower redshifts, $z \sim 2.7$, a conclusion independently reached by Gonzalez et al. (2008).

A comparison of the *HST* image at 606 nm and *Spitzer* images at 3.6 and 8.0 μm shows that two optical sources of different

[1] Obtained using ADDSCAN/SCANPI process available through NASA/IPAC Infrared Science Archive (http://irsa.ipac.caltech.edu).

Table 2. Optical and IR photometry of galaxies within the positional uncertainty of MMJ0659−557. Sources A–E refer to those objects identified in Fig. 4. All fluxes are given in μJy. Redshifts with superscripts *p* denote photometric-redshift estimates (this paper), and with *s* denotes a spectroscopic redshift from Barrena et al. (2002).

Source	Redshift	606 nm	775 nm	3.6 μm	4.5 μm	5.8 μm	8.0 μm	Notes
A	–	0.8 ± 0.05	1.0 ± 0.03					
B	–	0.6 ± 0.05	1.3 ± 0.03					
C	2.7 ± 0.2^{p}			27 ± 1	44 ± 1	57 ± 7	54 ± 2	After E subtraction
D	2.7 ± 0.2^{p}			25 ± 2	41 ± 1	80 ± 8	100 ± 2	After E subtraction
E	0.297^{s}	63 ± 4	80 ± 4	192 ± 12	135 ± 9	112 ± 5	75 ± 4	

morphologies (objects A and B in Fig. 4) lie ≤ 2 arcsec to the south of the IR centroids of objects C and D, which are most clearly defined in the 8.0 μm image. A small positional offset of RA $= -0\farcs4$, Dec. $= 0\farcs0$ was applied to the archival *HST* data to align it with the IRAC image. The error in this offset, determined from the registration of stars detected in both fields, is insufficient to account for the apparent separation of the IR and optical pairs of galaxies. Before considering further the possibility of the association of the IR sources C and D with the optical *HST* sources A and B, and collectively all four sources with MMJ065837−5557.0, we present an estimate of the photometric redshifts of the two IR sources.

3.4 IR photometry, colours and photometric redshifts

The difference in resolution between optical *HST* and IR *Spitzer* observations is significant. While the two extended red *Spitzer* sources (C and D) are clearly seen in the original 8 μm IRAC images, the halo of the elliptical galaxy (object E in Fig. 4) makes it non-trivial to measure their IR colours. Furthermore it is difficult to unambiguously determine if the IR emission of source C is associated with the optical emission of A, and similarly the IR source D with that of the optical source B. To minimize the contamination of the elliptical galaxy on the extracted fluxes of sources A, B, C and D, we model the elliptical galaxy using a two-dimensional light-profile fit to the high-resolution *HST* image at 606 nm. A subtraction of this model from the corresponding 775 nm data did not reveal any significant residuals at the position of the elliptical. This same model was then smoothed and scaled to the resolution and peak intensity of the elliptical galaxy emission in all four *Spitzer* IRAC bands and subtracted from each IRAC image, producing smooth residuals at the centre of the elliptical that matched the surrounding sky values. The optical fluxes at 606 and 775 nm for sources A and B were obtained using 1.5 and a 1.0 arcsec radius aperture photometry, respectively, and adopting sky values estimated from concentric 0.5 arcsec width rings, after masking any prominent objects, like star S. The IR fluxes for sources C and D at 3.6, 4.5, 5.8 and 8.0 μm were extracted via aperture photometry after subtraction of the elliptical galaxy, as explained above. Star S was also modelled by a PSF, scaled and subtracted from the images to produce smooth profiles of the underlying object D, without creating large residuals in its structure. Sky values were estimated from areas without contamination of faint objects within concentric 3–8 pixel rings multiple times, and 2.5–3.0 pixel (3.0–3.6 arcsec) radial aperture photometry was performed for each estimated sky value, and corrected to account for flux losses using the PSF model corrections of the IRAC Data Handbook version 3.0. No attempt was made to formally measure the errors introduced in the photometry due to the elliptical and star subtractions, since the limited resolution of the IRAC images is not sufficient to constrain subpixel positional accuracies. Since both C and D lie outside the centroid of E and S, these additional errors are estimated to be less than 10 per cent. All derived fluxes are listed in Table 2.

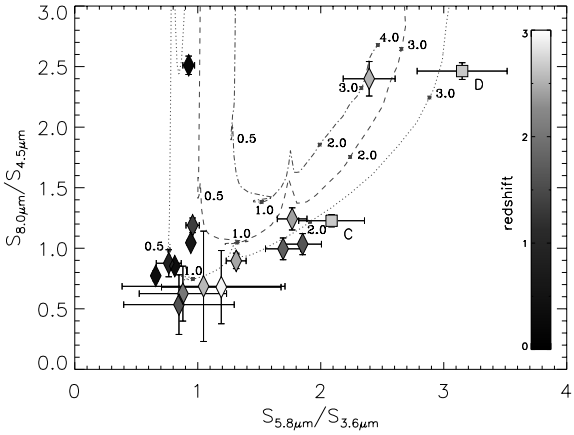

Figure 6. Colour–colour plot of IRAC-detected submillimetre galaxies in the GOODS-N (Pope et al. 2006), SHADES SXDF (Clements et al. 2008) and Lockman–Hole fields (Dye et al. 2008) with secure spectroscopic redshifts, represented as diamonds, where the hue of the symbols is proportional to the redshifts. SXDF850.21, at $S_{8.0\,\mu m}/S_{4.5\,\mu m} = 8.27$, $S_{5.8\,\mu m}/S_{3.6\,\mu m} = 1.33$, $z_{spec} = 0.044$ is out of bounds of the represented plot, but has been included in the analysis. The squares represent the two IR bright components (C and D) that are possible counterparts at $z \sim 2.7$ to MMJ065837−5557.0. The lines represent the colour changes for three model SEDs of dusty galaxies (Siebenmorgen & Krügel 2007) placed at increasingly larger redshifts, as indicated by the small labels.

Fig. 6 shows an IRAC colour–colour plot, $S_{8.0\,\mu m}/S_{4.5\mu m}$ versus $S_{5.8\,\mu m}/S_{3.6\,\mu m}$, for IRAC-detected SMGs in the GOODS-N (Pope et al. 2006), Subaru-XMM Deep Field (Clements et al. 2008), and Lockman Hole (Dye et al. 2008) fields, along with the location of sources C and D. Both sources have IR colours consistent with other known SMGs.

A crude photometric redshift for MMJ065837−5557.0 can be estimated, based on the IRAC photometry, using an empirical polynomial fit to the colours of similar galaxies. This technique has been used successfully in the optical and IR for various galaxy populations (e.g. Connolly et al. 1995 and Pope et al. 2006). We adopt a functional form $z = a + \sigma\, b_i \log S_i$, where a and b_i are coefficients that are fit to the appropriate galaxy population (SMGs in this case), and S_i are the IRAC flux densities of the training galaxies at 3.6, 4.5, 5.8 and 8.0 μm. We fit our model to the IR colours of the 16 SMGs with unambiguous single optical/IR counterparts, complete IRAC photometry, and robust spectroscopic redshifts in the GOODS-N and SCUBA Half Degree Extragalactic Survey (SHADES) fields (Pope et al. 2006; Dye et al. 2008; Clements et al. 2008). A best-fitting results in the relationship

$$z = 1.6393 + 3.9134 \log(S_{5.8}/S_{3.6}) - 2.3490 \log(S_{8.0}/S_{4.5}). \quad (1)$$

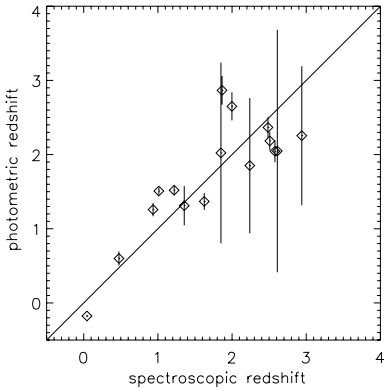

Figure 7. Photometric versus spectroscopic redshift of submillimetre galaxies in the GOODS-N and SHADES fields. The photometric redshift for each galaxy has been calculated using an empirical fit to the colours of SMGs, following the method described in Section 3.3. The dispersion of values between spectroscopic and photometric redshifts is $\langle \delta z/(1+z) \rangle = 0.15$.

In order to test the accuracy of this photometric-redshift estimate for the SMG population we use a *leave-one-out cross validation* technique, where each member of the training-galaxy set is systematically excluded from the fit, and then that best-fitting solution is used to derive its photometric redshift. This ensures that the accuracy of this photometric redshift technique is determined independently of the galaxies used to derive it. Fig. 7 shows the comparison of the spectroscopic redshifts of the training set to the photometric redshifts derived from the IRAC colours. We estimate the error in each photometric redshift by bootstrapping on the photometric errors in the colours. We find an average error between photometric and spectroscopic redshifts of $\langle \delta z/(1+z) \rangle = 0.15$ for this technique. Although the accuracy of this method decreases as the redshift increases, at least based on this small sample, there is no apparent bias to it.

Using this technique, we find that both IR sources, C and D, have photometric redshifts of 2.7 ± 0.2 where the uncertainty is derived from the observed colours of the galaxies and bootstrapping on their individual errorbars. This supports the arguments that they are either multiply lensed images of the same source or two galaxies separated (in the image plane) by ∼35 kpc and are undergoing an interaction that stimulates star formation in dust-obscured regions.

3.5 Counterparts to MMJ065837−5557.0

We now explore a number of scenarios regarding the possible associations of the optical and IR sources A, B, C and D (Fig. 4).

Scenario 1: Gradients of patchy dust obscuration (A = C and B = D). If we assume that the optical *HST* and IR *Spitzer* emission of components A and C, and similarly for components B and D, arises from different and distinct regions of the same galaxy, and that the galaxies A/C and B/D are both at redshifts $z \sim 2.7$ (Section 3.4), then the physical separations of the IR and optically emitting regions in each galaxy are <16 kpc in the plane of the lens. We consider how this apparent separation decreases in the source plane. Using previously published mass models derived from strong lensing data alone (Mehlert et al. 2001) along with combined strong and weak-lensing reconstruction for the cluster 1E0657−558 (Bradač et al. 2006), the image plane is mapped back to the source plane using the inversion software LENSTOOL (Jullo et al. 2007). We model the Bullet Cluster as two large-scale smooth potentials, and include the elliptical galaxy, a confirmed cluster member, as an additional small-scale local perturber. Following Bradač et al. (2006), the main cluster is modelled with a surface mass density (or convergence) $\kappa(r) \propto r^{-1.2}$ and velocity dispersion $\sigma \sim 1400\,\mathrm{km\,s^{-1}}$, whilst the subcluster has a slightly shallower slope of $\kappa\ (r) \propto r^{-0.9}$ and $\sigma \sim 1200\,\mathrm{km\,s^{-1}}$. Typically the local amplification, $\kappa^2 - \gamma^2$, where γ is the shear, provides an comparable expansion of the image plane compared to the source plane. In the vicinity of the MMJ065837−5557.0, however, the shear field of the cluster is perpendicular to the elongation of the cluster. Hence, adopting the above composite mass model, the ∼2 arcsec separation of the pairs of optical and IR galaxies (A/C and B/D) in the image plane is reduced only by a factor of 0.5–0.75, or a separation of 1.0–1.5 arcsec (10–13 kpc), in the source plane.

It is therefore possible that the galaxies identified in the *HST* image are the same as those detected by *Spitzer* IRAC, that is A = C and B = D, implying that the thermal emission at millimetre wavelengths arises from distant, dusty starburst galaxies with a gradient of heavy, but patchy obscuration. In support of this argument, recent *K*-band imaging of the same composite systems by Gonzalez et al. (2008) shows that the centroid of the 2.2 μm emission lies between the optical *HST* and longer wavelength 3–8 μm *Spitzer* data.

Scenario 2: Interacting pairs of red and blue galaxies (A ≠ C and B ≠ D). Alternatively, the *HST* and *Spitzer* data may be indicating that we have two close pairs of strongly interacting or merging galaxies, in which each pair contains an optical galaxy and an IR dust-obscured starburst. The observed separation of sources A and C (and equivalently B and D), that is ∼8 arcsec, corresponds to ≤30 kpc in source plane. The association of composite (possibly interacting) systems, red galaxies and blue companions, with the environments of SMGs is not uncommon (Ivison et al. 2002). The *Antennae* galaxy provides an excellent local example of the complex wavelength-dependent morphology in a merging galaxy with spatially distinct regions of luminous optical emission from young stars, and even greater luminosity at millimetre wavelengths originating from a young starburst population that remains heavily embedded in the dusty, gas-rich interstellar medium (see for example Whitmore et al. 1999; Xu et al. 2000; Wang et al. 2004).

Scenario 3: Two multiple lensed images of a background galaxy (A = B = C = D). The final scenario that we consider, which is consistent with the cluster lens model, is one in which the pairs of optical and IR galaxies are bisected by a critical line of infinite magnification. In this case, objects A, B, C and D may all be multiple lensed images of the same background source. Similar examples are presented by Kneib et al. (2004) and Borys et al. (2004) in the clusters Abell 2218 ($z = 0.17$) and MS0451.6−0305 ($z = 0.55$), respectively. In these cases bright submillimetre sources detected by SCUBA (9–17 mJy at 850 μm) are associated with multiple images of highly magnified, multi-component optical and IR galaxies which are bisected by the critical lines. After demagnification, the intrinsic fluxes of these particular SMGs are 0.4–0.8 mJy at 850 μm, making them some of the faintest SMGs detected to date.

An argument against the optical sources A and B being multiple images of the same background galaxy is that they have different morphologies in the high-resolution *HST* observations (Fig. 4). Source A shows more extended and elongated emission than source B, which appears to consist of two compact emitting areas. However, the presence of the cluster-member elliptical galaxy (source E in Fig. 4) is able to provide sufficient gravitational mass to distort the resolved optical images and create additional magnification of the background source (e.g. Natarajan & Kneib 1997). It is not necessary therefore that the two lensed images of the background source should have identical magnifications and morphologies. Given the

optical brightness of galaxies A and B, this scenario can be easily tested via a spectroscopic determination of their redshifts.

Finally, we mention that our gravitational-lens model also predicts a third counterpart to the multiply imaged background source with only a modest magnification factor of 3–5 at $06^{h}58^{m}33^{s}.5$, $-55^{d}57^{m}29^{s}$ (J2000). A faint red IRAC source is seen at this position with no optical counterpart. We do not discuss the possibility of this third source further, except to mention that it is marginally consistent with the orientation of the slightly extended profile of the millimetre emission from MMJ065837−5557.0.

Regardless of the degree of association between the IR and optical sources, the IRAC photometric redshifts are well-within the redshift distribution of the blank-field SMG population, and thus we believe that the most plausible explanation for the millimetre-wavelength flux is that (1) the AzTEC source MMJ065837−5557.0 lies behind the Bullet Cluster, (2) it is lensed by the Bullet Cluster and (3) it is a product of the combined emission of the IRAC objects C and D. This scenario also naturally explains the approximate equal distance from the AzTEC centroid position to the two IR galaxies. In the absence of a detailed lensing model in the vicinity of the AzTEC source and/or spectroscopic confirmation, we assume in the remainder of this paper that both pairs of optical/IR sources (A/C and B/D) are associated with MMJ065837−5557.0, which is a lensed background SMG.

3.6 Contribution of the Sunyaev–Zel'dovich effect to the observed flux of MMJ065837−5557.0

Two classes of effects can serve to increase the measured brightness of detected point sources: multiplicative effects (lensing) and additive contributions to the flux due to millimetre-wavelength emission along the line of sight to the source. MMJ065837−5557.0 clearly suffers from both. In this section we describe the non-negligible millimetre-wavelength emission due to the thermal Sunyaev-Zel'dovich Effect (SZE, Sunyaev & Zeldovich 1970, 1972) that is added to the intrinsic lensed emission of MMJ065837−5557.0. The thermal SZE is produced by inverse-Compton scattering of the cosmic microwave background (CMB) photons off electrons in the hot and dense intercluster medium (ICM) of clusters. We do not consider the contribution from the weaker kinetic SZE that is due to the bulk motion (velocity) of the cluster plasma with respect to the CMB reference frame. Consequently the thermal SZE is a dominant source of secondary fluctuations on the surface brightness of the CMB on small angular scales, less than a few arcminutes.

Unable to perform a multi-wavelength spectral decomposition of the SZE and the bright background galaxy MMJ065837−5557.0, with AzTEC observations only at 1.1 mm, we can estimate the level of the thermal SZE contamination in two independent ways.

First, taking advantage of the spatial resolution of the AzTEC observations and assuming that the SZE emission from the cluster is smooth on spatial scales smaller than that of the AzTEC beam (30 arcsec), we can spatially filter the AzTEC map and fit for the 1.1 mm flux consistent with only point-source emission (as discussed in Section 2.1). Alternatively, as described below, we can model the SZE emission from the Bullet Cluster with a simple model for the electron temperature and density distribution to estimate the 1.1 mm flux from the SZE at the position of the AzTEC point source.

The derivation of the intensity of the SZE and its observed properties at radio to millimetre-wavelengths have been reviewed extensively (Sunyaev & Zeldovich 1980; Birkinshaw 1999; Carlstrom, Holder & Reese 2002; Birkinshaw & Lancaster 2007). Briefly, considering only the thermal distortion, the frequency-dependent SZE is given by the simple expression

$$\delta I_{\nu} = I_0[g(x)y], \tag{2}$$

where $I_0 = 2\,(k_B T_0)^3/(hc)^2$ and $T_0 = 2.725$K is the mean temperature of the CMB. The Comptonization parameter, y, equal to the optical depth times the fractional energy gain of each scattering event, is

$$y = \frac{k_B \sigma_T}{m_e c^2} \int n_e T_e \, \mathrm{d}l. \tag{3}$$

Finally, the dimensionless spectral function, $g(x)$, where $x = h\nu/k_B T_0$, describes the frequency dependence of the thermal SZE. Neglecting relativistic corrections, $g(x)$ has the form

$$g(x) = \frac{x^4 \mathrm{e}^x}{(\mathrm{e}^x - 1)^2} \left(x \frac{\mathrm{e}^x + 1}{\mathrm{e}^x - 1} - 4 \right). \tag{4}$$

Since the intensity of SZE is dependent only on the line-of-sight integral of the electron pressure through the Bullet Cluster, we describe below our estimations for the local value of the electron temperature and density at the position of MMJ065837−5557.0.

It is common to adopt an isothermal assumption within the cluster density distribution (typically a β model), or at least a weak radial dependence on the temperature of the intracluster medium within the virial radius (Irwin, Bregman & Evrard 1999). Support for this assumption is also found in hydrodynamical simulations (Eke, Navarro & Frenk 1998; Pearce et al. 2000). In the case of the Bullet Cluster, Markevitch et al. (2002) have provided a temperature map that shows a gas–temperature variation across the merging clusters between 10–24 keV, ignoring the concentrated cold spot or 'bullet' (with a temperature of 6–7 keV). The spatial resolution of AzTEC (30 arcsec FWHM beamsize) is sufficient to estimate that the local temperature of the X-ray-emitting gas, at the position of MMJ065837−5557.0, is 14–16 keV (regions f–g in fig. 2 of Markevitch et al. 2002), or similar to the average cluster temperature of ∼15 keV.

Whilst the density profile of the gas to the west of the main X-ray peak (in the direction of the 'bullet') requires the inclusion of a shock front and an additional component to represent the lower mass merging cluster, the situation is less complicated to the east of the X-ray peak brightness, in the direction of MMJ065837−5557.0. The local electron density, n_e, in the eastern hemisphere (at the position of MMJ065837−5557.0) is calculated using a single-component spherically symmetric β model ($\beta = 0.7$) centred at the primary peak of the observed X-ray surface-brightness distribution. We begin by considering a range for the total cluster mass, $M_{\rm tot} = 0.8$–$1.9 \times 10^{15}\,\mathrm{M}_{\odot}$ (Clowe et al. 2006; Vikhlinin et al. 2006). Following Kay, Liddle & Thomas (2001) we then assume that the ICM is fully ionized, with a helium mass fraction of 0.24, such that $n_e = 0.88\rho/m_{\rm H}$, where $m_{\rm H}$ is the mass of a hydrogen atom. The baryonic mass density, ρ, is calculated assuming a global baryon fraction $f_b = M_b/M_{\rm tot} = 0.06\,h^{-3/2}$ (Ettori & Fabian 1999). The exercise was then repeated assuming an alternative β model centred on the peak of the weak-lensing signal from the main cluster that dominates the total cluster mass (Section 3.3). Finally, provided that the electron temperature, T_e, is similar to the X-ray gas temperature, we determine that the contribution of the SZE at 1.1 mm at the position of the AzTEC point-source MMJ065837−5557.0 is ∼1.5–4.2 mJy beam^{-1}. This estimated range of underlying flux due to the SZE is consistent with what we measure directly from the extended component in the spatially resolved 1.1 mm emission at the position of the AzTEC point source (Section 2.1).

We therefore conclude that the 1.1 mm flux density of MMJ065837−5557.0 due solely to continuum emission from a lensed high-redshift SMG is in the range 12–14 mJy. An analysis of the detected extended AzTEC emission towards the Bullet Cluster (Ezawa et al. in preparation) will provide more accurate information on the location of MMJ065837−5557.0 with respect to the peak of the SZE, and consequently a more accurate measurement of the point-source contamination to the integrated SZE (a potential problem for lower resolution experiments) than the estimate described above.

Assuming a range of spectral indices $\alpha \sim 3$–4 (where $F_\nu \propto \nu^\alpha$) and dust temperatures to describe the rest-frame SED of MMJ065837−5557.0 in the millimetre regime, we also determine that MMJ065837−5557.0 is too faint to be detected in the low-resolution (FWHM ~ 4.5 arcmin) ACBAR observations at 1.4 mm given the published noise level of 30 μK (Gomez et al. 2004). This is consistent with the lack of comment by Gomez et al. about a detectable signal at the null frequency of the SZE.

3.7 The intrinsic luminosity of MMJ065837−5557.0 – a dusty high-redshift LIRG

The magnification map of the Bullet Cluster by Mehlert et al. (2001) suggests a robust and conservative lower limit of $A = 20$ for the amplification of MMJ065837−5557.0. More typical amplifications of $A = 1$–3 have been found for SMGs behind low-z massive clusters (Ledlow et al. 2002; Knudsen et al. 2006). It is the proximity of MMJ065837−5557.0 to a lensing caustic line that makes this such an exceptional case. The implication for such a large magnification is that the AzTEC source has an intrinsic flux of $S_{1.1\,\mathrm{mm}} < 0.68$ mJy, after subtraction of the expected contribution from the Sunyaev-Zel'dovich effect. This is a factor of >3 lower than the flux of the faintest blank-field SMGs detected in the full 225 arcmin^2 AzTEC field towards the Bullet Cluster (which occupies only the central 12 arcmin^2).

Assuming that the AzTEC point source is a background galaxy at $z \sim 2.7$, then intrinsic millimetre-wavelength brightness of MMJ065837−5557.0, after the corrections for the SZE contribution and amplification, corresponds to a far-IR (FIR) luminosity of $<10^{12}\,L_\odot$. Given the relative insensitivity of the millimetre-wavelength flux density as a function of redshift, this is a robust result provided that the AzTEC source lies in the redshift range $\sim 1 < z < 8$. Hence, rather than having discovered an extremely rare example of a hyperluminous dust-obscured galaxy, MMJ065837−5557.0 is more typical of a LIRG with $L_{\mathrm{FIR}} \leq 10^{11}$–$10^{12}\,L_\odot$ in the high-redshift Universe, with a star-formation rate (SFR) in the range 5–50 $M_\odot\,\mathrm{yr}^{-1}$ (Kennicutt 1998).

The conservative lower limit on the magnification implies that even a more modest SFR may be appropriate, closer to that of only a mildly active starburst galaxy. This would support the scenario in which the millimetre emission arises from a distant starburst with patchy dust obscuration and a low dust content, which in turn increases the likelihood of detecting both the optical and IR emission from the source (i.e. A/C and/or B/D). Only high-resolution (sub)millimetre interferometric imaging of MMJ065837−5557.0, to unambiguously identify the counterpart(s), combined with spectroscopic measurements to determine the redshifts (and possibly velocity dispersion) of all optical and IR components (A, B, C, D) will allow progress in understanding the nature of this potentially rare example of a low to intermediate luminosity millimetre-selected galaxy in the high-redshift Universe.

4 CONCLUSIONS

Sensitive continuum observations at 1.1 mm with the AzTEC camera installed on the 10-m diameter Atacama Submillimeter Telescope Experiment have been made towards the Bullet Cluster. An extremely bright point source (MMJ065837−5557.0) is detected with an observed flux density at 1.1 mm of 15.9 mJy. The centroid position of MMJ065837−5557.0 lies close to the largest mass-density peak in the weak-lensing map of Clowe et al. (2006).

Archival IR (*Spitzer* IRAC) images show the presence of two red sources, separated by ∼8 arcsec (or ≤30 kpc in the source plane), that lie within the positional error of MMJ065837−5557.0, and that also straddle the critical magnification line (i.e. a region of extreme amplifications) of Mehlert et al. (2001). The *Spitzer* IRAC colours of these two sources are typical of high-z SMGs, and photometric-redshifts place both sources at $z \sim 2.7 \pm 0.2$. The proximity of *HST*-identified optical sources to both of these *Spitzer* IRAC galaxies leaves open 2 possibilities: (1) that each optical/IR pair are individual galaxies undergoing close interaction or (2) that each pair is in fact only one galaxy with a complex morphology of patchy dust obscuration.

Having rejected a Galactic origin and a cluster member origin as the source of the AzTEC emission, the above conditions suggest that MMJ065837−5557.0 is a background source associated with one or both of the red IR *Spitzer* sources, and is strongly lensed by this massive cluster. The agreement in the location of the critical line in the magnification maps of Mehlert et al. (2001), Bradač et al. (2006) and Gonzalez et al. (2008) for this cluster place a strong conservative limit of >20 for the magnification of the millimetre emission from MMJ065837−5557.0. There exist many similarities between this example of an extremely bright millimetre source and the possibility of gravitationally lensed interacting galaxies that produce a bright submillimetre arc in MS0451.6−0305 (Borys et al. 2004).

After subtracting the contribution (≤25 per cent) due to the extended SZE at 1.1 mm from the total AzTEC continuum flux of MMJ065837−5557.0, we estimate that the intrinsic (i.e. demagnified) FIR luminosity of MMJ065837−5557.0 is $<10^{12}\,L_\odot$ provided the source lies in the redshift range $\sim 1 < z < 8$. Hence, MMJ065837−5557.0 is representative of the fainter population of star-forming galaxies that is undetectable, without the assistance of lensing, with the current generation of small single-dish (sub)millimetre telescopes due to source confusion and lack of sensitivity. Until the commissioning of the next generation of larger millimetre-wavelength facilities (e.g. LMT, ALMA) the only opportunity to study this fainter luminosity class of IR galaxies, that dominate the production of the cosmic IR background, is to take advantage of the significant amplification that exist towards the critical magnification lines of massive nearby clusters.

ACKNOWLEDGMENTS

We thank the referee for the thorough reading and suggestions to improve the paper, and also Jack Hughes for useful comments. We recognize and thank Douglas Clowe for valuable discussions during the early preparation of this paper. This study was financially supported by MEXT Grant-in-Aid for Scientific Research on Priority Areas No. 15071202, by the Grant-in-Aid for the Scientific Research from the Japan Society for the Promotion of Science (No. 19403005), by NSF Grant no. 0540852, and CONACYT grants no. 50786 and 60878. Some of the data analyzed in this paper were obtained from the Multimission Archive at the Space Telescope Science Institute (MAST) and the *Spitzer* Space Telescope archive.

STScI is operated by the Association of Universities for Research in Astronomy, Inc., under NASA contract NAS5−26555. The *Spitzer* Space Telescope is operated by the Jet Propulsion Laboratory, California Institute of Technology, under a contract with NASA. This research has made use of NASA's Astrophysics Data System.

REFERENCES

Aretxaga I., Hughes D. H., Chapin E. L., Gaztañaga E., Dunlop J. S., Ivison R. J., 2003, MNRAS, 342, 759
Aretxaga I., Hughes D. H., Chapin E. L., Gaztañaga E., Dunlop J. S., Ivison R. J., 2007, MNRAS, 379, 1571
Barrena R., Biviano A., Ramella M., Falco E. E., Seitz S., 2002, A&A, 386, 816
Bertoldi F. et al., 2007, ApJ, 172, 132
Birkinshaw M., 1999, Phys. Rep., 310, 97
Birkinshaw M., Lancaster K., 2007, New Astron. Rev., 51, 346
Borys C. et al., 2004, MNRAS, 352, 759
Bradač M. et al., 2006, ApJ, 652, 937
Carlstrom J. E., Holder G. P., Reese E. D., 2002, ARA&A, 40, 643
Chapman S. C., Smail I., Ivison R. J., Blain A. W., 2002, MNRAS, 335, L17
Chapman S. C., Blain A. W., Ivison R. J., Smail I. R., 2003, Nat, 422, 695
Chapman S. C., Blain A. W., Smail I., Ivison R. J., 2005, AJ, 622, 772
Clements D. et al., 2008, MNRAS, 387, 247
Clowe D., Bradač M., Gonzalez A. H., Markevitch M., Randall S. W., Jones C., Zaritsky D., 2006, AJ, 648, L109
Connolly A. J., Csabai I., Szalay A. S., Koo D. C., Kron R. G., Munn J. A., 1995, AJ, 110, 2655
Coppin K. et al., 2006, MNRAS, 372, 1621
Cowie L. L., Barger A. J., Kneib J.-P., 2002, AJ, 123, 2197
Dye S. et al., 2008, MNRAS, 386, 1107
Eke V. R., Navarro J. F., Frenk C. S., 1998, AJ, 503, 569
Ettori S., Fabian A. C., 1999, MNRAS, 305, 834
Ezawa H., Kawabe R., Kohno K., Yamamoto S., 2004, in Oschmann J. M., Jr, ed., Proc. SPIE Vol. 5489, Ground-based Telescopes. SPIE, Bellingham, p. 763
Gomez P. et al., 2004, in Bertin G., Farina D., Pozzoli R., eds, AIP Conf. Ser. Vol. 703, Plasmas in the Laboratory and in the Universe: New Insights and New Challenges. Am. Inst. Phys., New York, p. 361
Gonzalez A. H., Clowe D., Bradac M., Zaritsky D., Jones C., Markevitch M., 2008, ApJ, submitted (arXiv:0803.3794)
Greve T. R., Ivison R. J., Bertoldi F., Stevens J. A., Dunlop J. S., Lutz D., Carilli C. L., 2004, MNRAS, 354, 779
Griffin M. J., Orton G. S., 1993, Icarus, 105, 537
Hibbard J. E., Yun M. S., 1999, ApJ, 522, L93
Irwin J. A., Bregman J. N., Evrard A. E., 1999, ApJ, 519, 518
Ivison R. J., Smail I., Le Borgne J.-F., Blain A. W., Kneib J.-P., Bezecourt J., Kerr T. H., Davies J. K., 1998, MNRAS, 298, 583
Ivison R. J. et al., 2002, MNRAS, 337, 1
Jullo E., Kneib J.-P., Limousin M., Elíasdóttir Á., Marshall P. J., Verdugo T., 2007, New J. Phys., 9, 447
Kay S. T., Liddle A. R., Thomas P. A., 2001, MNRAS, 325, 835
Kennicutt R. C. Jr, 1998, ARA&A, 36, 189
Kneib J.-P., van der Werf P. P., Kraiberg Knudsen K., Smail I., Blain A., Frayer D., Barnard V., Ivison R., 2004, MNRAS, 349, 1211
Knudsen K. K. et al., 2006, MNRAS, 368, 487
Laurent G. T. et al., 2005, ApJ, 623, 742
Ledlow M. J., Smail I., Owen F. N., Keel W. C., Ivison R. J., Morrison G. E., 2002, ApJ, 577, L79
Markevitch M., Gonzalez A. H., David L., Vikhlinin A., Murray S., Forman W., Jones C., Tucker W., 2002, ApJ, 567, L27
Mehlert D. et al., 2001, A&A, 379, 96
Natarajan P., Knieb J.-P., 1997, MNRAS, 287, 833
Nusser A., 2008, MNRAS, 384, 343
Pearce F. R., Thomas P. A., Couchman H. M. P., Edge A. C., 2000, MNRAS, 317, 1029
Perera T. A. et al., 2008, MNRAS, submitted (arXiv:0806.3791)
Polletta M. et al., 2007, ApJ, 663, 81
Pope A., Borys C., Scott D., Conselice C., Dickinson M., Mobasher B., 2005, MNRAS, 358, 149
Pope A. et al., 2006, MNRAS, 370, 1185
Romero G. E., Combi J. A., Colomb F. R., 1994, A&A, 288, 731
Scott K. S. et al., 2008, MNRAS, 385, 268
Siebenmorgen R., Krügel E., 2007, A&A, 461, 445
Smail I., Ivison R. J., Blain A. W., 1997, AJ, 490, L5
Smail I., Ivison R. J., Blain A. W., Kneib J.-P., 2002, MNRAS, 331, 495
Stevens J. A. et al., 2003, Nat, 425, 264
Sunyaev R. A., Zeldovich Y. B., 1970, Comments Astrophys. Space Phys., 2, 66
Sunyaev R. A., Zeldovich Y. B., 1972, Comments Astrophys. Space Phys., 4, 173
Sunyaev R. A., Zeldovich I. B., 1980, ARA&A, 18, 537
Vikhlinin A., Kravtsov A., Forman W., Jones C., Markevitch M., Murray S. S., Van Speybroeck L., 2006, ApJ, 640, 691
Wang Z. et al., 2004, ApJ, 154, 193
Whitmore B. C., Zhang Q., Leitherer C., Fall S. M., Schweizer F., Miller B. W., 1999, AJ, 118, 1551
Wilson G. W. et al., 2008, MNRAS, 386, 807
Xu C., Gao Y., Mazzarella J., Lu N., Sulentic J. W., Domingue D. L., 2000, ApJ, 541, 644
Yun M. S. et al., 2008, MNRAS, 389, 333

This paper has been typeset from a TEX/LATEX file prepared by the author.